Environmental Pollution 275 (2021) 116665

Contents lists available at ScienceDirect

Environmental Pollution

journal homepage: www.elsevier.com/locate/envpol

Metabolomics reveals the reproductive abnormality in female zebrafish exposed to environmentally relevant levels of climbazole☆

Ting Zou [a, 1], Yan-Qiu Liang [b, 1], Xiaoliang Liao [a], Xiao-Fan Chen [a], Tao Wang [c], Yuanyuan Song [c], Zhi-Cheng Lin [a], Zenghua Qi [a], Zhi-Feng Chen [a, d, *], Zongwei Cai [a, c]

[a] Guangdong Key Laboratory of Environmental Catalysis and Health Risk Control, School of Environmental Science and Engineering, Institute of Environmental Health and Pollution Control, Guangdong University of Technology, Guangzhou, 510006, China
[b] Faculty of Chemistry and Environmental Science, Guangdong Ocean University, Zhanjiang, 524088, China
[c] State Key Laboratory of Environmental and Biological Analysis, Department of Chemistry, Hong Kong Baptist University, Hong Kong Special Administrative Region, China
[d] Guangdong Provincial Key Laboratory of Chemical Pollution and Environmental Safety, South China Normal University, Guangzhou, 510006, China

ARTICLE INFO

Article history:
Received 15 November 2020
Received in revised form
10 January 2021
Accepted 2 February 2021
Available online 5 February 2021

Keywords:
Azole fungicide
Zebrafish
Metabolomics
Reproductive toxicity
Oxidative stress

ABSTRACT

Climbazole (CBZ) ubiquitously detected in the aquatic environment may disrupt fish reproductive function. Thus far, the previous study has focused on its transcriptional impact of steroidogenesis-related genes on zebrafish, but the underlying toxic mechanism still needs further investigation at the metabolic level. In this study, adult zebrafish were chronically exposed to CBZ at concentrations of 0.1 (corresponding to the real concentration in surface water), 10, and 1000 μg/L and evaluated for reproductive function by egg production, with subsequent ovarian tissue samples taken for histology, metabolomics, and other biochemical analysis. After 28 days' exposure, fecundity was significantly decreased in all exposure groups, with the inhibition of oocytes in varying developmental stages to a certain degree. The decrease in retinoic acid and sex hormones, down-regulated genes important in steroidogenesis, and increase in oxidized/reduced glutathione ratio and occurrence of apoptotic cells were observed in zebrafish ovaries following exposure to CBZ even at environmentally realistic concentrations, suggesting that alternations in steroidogenesis and oxidative stress can play significant roles in CBZ-triggered reproductive toxicity. Besides, mass spectrometry imaging analysis validated the results from metabolomics analysis. Our findings provide novel perspectives for unveiling the mechanism of reproductive dysfunction by CBZ and highlight its risk to fish reproduction.

1. Introduction

Azole fungicides are antifungal agents with at least one five-membered heterocyclic ring containing two or three nitrogen atoms in their structures. Their antifungal activities are based on the combination of N-3 (imidazole) or N-4 (triazole) substituent of the azole ring with the haem of the enzyme sterol 14α-demethylase (encoded by *cyp51*); so that azole fungicides can hinder the biosynthesis of the essential cell membrane component and eventually inhibit the growth of fungi (Chen and Ying, 2015). On account of their excellent fungicidal abilities, azole fungicides are extensively used in pharmaceuticals and personal care products; for example, climbazole (CBZ) is most commonly found as an anti-dandruff antifungal active ingredient in rinse-off hair products (e.g., shampoos) and as a preservative in leave-on cosmetics (e.g., face cream, hair location, and foot care). In 2017, the Scientific Committee on Consumer Safety (SCCS) reassessed the margin of safety for human health and concluded a reduction in the maximum concentrations of CBZ for use in different product types (SCCS, 2017). In addition to human safety, the CBZ residue in the environment could pose medium risks to aquatic organisms (Chen and Ying, 2015); accordingly, its environmental impacts should be of concern.

The annual usage of CBZ was reported in the range of 100–1000 tons in the European Union and calculated to be 345 tons in China

☆ This paper has been recommended for acceptance by Sarah Harmon.
* Corresponding author. Guangdong University of Technology, Guangzhou, China.
E-mail address: chenzhf@gdut.edu.cn (Z.-F. Chen).
[1] These authors contributed equally.

https://doi.org/10.1016/j.envpol.2021.116665
0269-7491/

(ECHA, 2013; Zhang et al., 2015). After use, CBZ could reach the aquatic environment because of direct or indirect discharge of wastewater (Chen et al., 2012, 2014; Liu et al., 2017). Our earlier study indicated that the mean and maximum concentrations of CBZ were 74.8 and 264 ng/L in surface water of the Dongjiang River, South China (Chen et al., 2014). A higher mean concentration of CBZ was found at 187 ng/L in the receiving water collected from the upstream and downstream sites of 100 m far from the outlet of ten wastewater treatment plants (Liu et al., 2017). Apart from its environmental levels, the acute toxicity of CBZ towards aquatic organisms covering different trophic levels has been studied; for instance, CBZ exhibited moderate toxicity on zebrafish (*Danio rerio*) embryos with a median lethal concentration (LC_{50}) of 8.20 mg/L (Richter et al., 2013). Although CBZ was not acutely toxic to zebrafish, we previously found the down-regulation of steroidogenesis-related genes in zebrafish eleutheroembryos after exposure to 100 ng/L of CBZ, which represents its environmentally relevant concentrations (Zhang et al., 2019a). There is growing evidence that azole fungicides could disrupt the endocrine system in female fish (Chu et al., 2016; Liao et al., 2014); however, the action mechanism remains unclear.

Reproductive toxicity refers to the adverse biological effects on the reproductive organs and related endocrine systems, such as interference in sexual function and fertility, associated with chemical substances. There are lots of reports regarding how environmental pollutants affect fish reproduction by commonly seen techniques, including enzyme-linked immunosorbent assay (ELISA) and quantitative real-time reverse transcription polymerase chain reaction (RT-qPCR) (Liang et al., 2020; Shi et al., 2018). These techniques focus on specific detection based on existing research results but are failing to discover unknown responses. Metabolomics is an emerging technique that analyzes the small-molecule metabolite profiles in a biological cell, tissue, organ, or organism and thereby provides an instantaneous snapshot of the physiology (Yan et al., 2020; Zhang et al., 2019b). In terms of toxicology, metabolomics can be used for large-scale screening of differential endogenous metabolites, reflecting the physiological changes, especially for ambiguous signaling pathways, in organisms caused by toxic chemicals, which is closely linked to the phenotypic changes (Fiehn, 2002; Jiang et al., 2019). Based on untargeted metabolomics analysis, certain azole fungicides reportedly regulated the levels of metabolites involving in energy metabolism, amino acids metabolism, lipid metabolism, nucleotide metabolism, cholesterol metabolism, and tricarboxylic acid cycle (Melvin et al., 2018; Teng et al., 2018). Besides, mass spectrometry imaging (MSI) is a supplementary tool for metabolomics analysis in recent years (Zhao et al., 2020b) with the advantages of visual determination of chemicals without extra labeling. The imaging approach has been effectively applied in metabolite distribution and biomarker discovery in tissues (Wei et al., 2020; Zhao et al., 2018), suggesting that the combined use of metabolomics and imaging could be more effectively used to reveal insights into the mechanism of toxicity.

The purpose of this study was to evaluate the reproductive effects on adult zebrafish chronically exposed to environmentally realistic concentrations of CBZ. First of all, the phenotypic endpoints, including egg production and ovarian histology, were analyzed. Secondly, untargeted metabolomics analysis was conducted to identify the differential signaling pathways in zebrafish ovaries preliminarily. Finally, a comprehensive analysis of sex hormone levels, mRNA expression, apoptosis, as well as metabolic imaging was performed to support the results from metabolomics analysis. Our results could provide insights into the mechanism of CBZ-induced reproductive toxicity on female zebrafish and emphasize the ecological risk of CBZ.

2. Materials and methods

2.1. Chemical and fish culture

Detailed information can be referred to Text S1.

2.2. Experimental design

After acclimation, healthy and uniform adult zebrafish (6 months old) were selected for exposure experiments. The zebrafish were randomly divided into four groups: a solvent control group (C-group, 0.001% DMSO), a low CBZ concentration group (L-group, 0.1 μg/L), a medium concentration group (M-group, 10 μg/L), and a high concentration group (1000 μg/L). One should be noted that the low exposure concentration of 0.1 μg/L is basically consistent with the CBZ level found in surface water samples collected from the Dongjiang River (Chen et al., 2014; Liu et al., 2017). Each group contained four replicates, and each replicate consisted of six pairs of females and males as breeding pairs. The experiment started with a pre-exposure period of 12 days to establish the baseline of egg production for each group, followed by a 28-day CBZ exposure period. The exposure experiment was conducted at a semi-static condition, and half of the exposure solutions were updated every 24 h. Water samples at the beginning of exposure (day 0) and before water renewal (day 1) were collected for CBZ concentration analysis, which was performed by our previous method with a little modification (Chen et al., 2012), with the detailed information provided in the Text S2 and Table S1. The eggs were collected and counted every day during the whole experimental period. Water quality parameters such as temperature, pH, and dissolved oxygen were measured periodically. After 28 days of exposure, the females were euthanized with ice, measured for wet weight, and then dissected immediately. The ovaries were isolated, weighed in order to assess the gonadosomatic index, and treated in different manners: fixed in 4% paraformaldehyde for the analysis of histology and apoptosis and preserved in RNAlater for transcriptional analysis. For mass spectrometry imaging analysis, the whole zebrafish was placed in a plastic rectangular mold with a 10% carboxymethyl cellulose (CMC) aqueous solution. All samples were stored at −80 °C for the subsequent determination.

2.3. Histological examination

The histological preparation of zebrafish ovaries was conducted as described previously (Liang et al., 2020). In brief, the fixed ovarian tissue samples (three replicates per group) were dehydrated through gradient ethanol, embedded in paraffin, and cut into 5 μm thick sections using an RM2016 microtome (Leica, China). The resultant sections were then dewaxed by xylene, dehydrated again, and finally stained with hematoxylin and eosin (H&E). The stained sections were recorded by an Eclipse E100 microscope (Nikon, Japan).

2.4. Metabolomics analysis

The metabolome extraction method was performed according to our previous studies with a slight modification (Yan et al., 2020; Zhang et al., 2019b). Firstly, the ovarian tissue samples (eight replicates per group) were combined with 500 μL of frozen methanol aqueous solution (80%, *v*/*v*) in centrifugal tubes, homogenized by a Jingxin JXFSTPRP-24 automatic grinder (Jingxin, China) at a constant frequency of 60 Hz for 10 s and followed by centrifugation (13,000×*g*, 10 min, 4 °C), after which the supernatants were collected and dried with gentle nitrogen. The obtained residuals were redissolved in 100 μL of methanol aqueous solution (50%, *v*/*v*).

Finally, the quality control (QC) sample was prepared by mixing 20 μL aliquots of solution from each sample in all groups.

The resultant samples were analyzed using an ultrahigh performance liquid chromatography system (UHPLC) coupled to a Q Exactive Focus Hybrid Quadrupole-Orbitrap Mass Spectrometer (QE Orbitrap MS) in both positive and negative ionization modes (Thermo Fischer Scientific, China). Details of instrumental parameters are listed in Table S2. The blank and QC samples were injected before and after the sample batch. Samples from the C-, L-, M-, and H-groups were loaded randomly, but a QC sample will be analyzed after every six samples. After peak deconvolution, peak normalization, disturbed signal exclusion, multivariate statistical analysis, metabolite identification, and pathway analysis, the significantly changed metabolites and signaling pathways between the control and exposure groups were structurally identified and proposed, respectively. Detailed data processing for metabolomics is described in Text S2.

2.5. Sex hormone measurement

Ovarian tissue samples (three replicates per group) were combined with phosphate-buffer saline (PBS, 1 mg tissue/10 μL PBS). After homogenization (60 Hz, 10 s), centrifugation (500×*g*, 20 min, 4 °C), and collection of the supernatant, the concentrations of sex hormones, including estradiol (E2), testosterone (T), and 11-ketotestosterone (11-KT), were detected by enzyme-linked immunosorbent assay (ELISA) using a commercial kit (J&L Biological). The detection limits of E2, T, and 11-KT were 0.05, 1.0, and 0.1 pg/mL, respectively.

2.6. RNA isolation and RT-qPCR analysis

Total RNA was extracted from ovarian tissue samples (three replicates per group) by TRIzol reagent (Invitrogen) according to the manufacturer's instruction. Detailed procedures regarding complementary DNA (cDNA) synthesis and RT-qPCR were described in our previous study (Text S2) (Zhang et al., 2019a). *β-actin* was selected as the housekeeping gene for normalization because of its high gene expression stability in zebrafish (Zhang et al., 2019a). The primer sequences of aromatase (*cyp19a1a*), steroid 17α-hydroxylase/17,20-lyase (*cyp17a1*), 17β-hydroxysteroid dehydrogenase 3 (*hsd17b3*), 20β-hydroxysteroid dehydrogenase (*hsd20b*), and 3β-hydroxysteroid dehydrogenase 1 (*hsd3b1*) genes, which are related to steroidogenesis, are listed in Table S3. Because of insufficient samples for transcriptional analysis, the transcripts of target genes in the L-group, representing environmentally realistic concentrations, were analyzed as a compromise. The fold changes in the relative mRNA expression were analyzed by a delta-delta comparative threshold cycle ($2^{-\Delta\Delta Ct}$) approach (Livak and Schmittgen, 2001).

2.7. TUNEL assay

Terminal deoxynucleotidyl transferase dUTP nick end labeling (TUNEL) assays were used to detect apoptotic cells by a commercial kit (Roche). Following the instruction, ovarian tissue sections (three replicates per group) were prepared as described in the histological examination, pretreated with protease K, and incubated with the fluorescein isothiocyanate (FITC) conjugated dUTP reagent for 2 h to detect DNA fragmentation. Finally, the cell nucleus was counterstained with DAPI dye. Fluorescein-labeled apoptotic cells were identified and photographed by observation with a fluorescent microscope (Nikon, Japan), and the positive apoptotic nucleus was green.

2.8. MALDI-MSI analysis

The frozen CMC block was removed from the plastic mold and continuously cryosectioned into 14 μm thick sagittal sections at −25 °C using an HM525 NX cryostat (Thermo Fischer Scientific, China). The frozen zebrafish slice was thaw-mounted on an indium-tin-oxide coated glass slide and dried in a vacuum desiccator for 30 min before matrix coating. The 2,5-dihydroxybenzoic acid (DHB) matrix solution was sprayed to the sections using an ImagePrep automatic matrix sprayer (Bruker Daltonics, Germany). Matrix-assisted laser desorption/ionization mass spectrometry imaging (MALDI-MSI) analysis was performed on an ultrafleXtreme II mass spectrometer (Bruker Daltonics, Germany) equipped with a smartbeam II laser. Instrumental conditions were set, as shown by our previous study (Text S2) (Wei et al., 2020). One sample per group was used in the MALDI-MSI analysis for the validation of metabolomics results. All data were analyzed by SCiLS Lab 2016a software. Data processing underwent weak denoising, the normalization of total ion count, and box-plot analysis.

2.9. Statistical analysis

All data were expressed as mean ± standard deviation. Statistical analysis was performed using GraphPad Prism 7.0 and SIMCA-P 14.1 software. In order to compare the exposure group to the control group, the significance of differences in the body weight, ovary weight, gonadosomatic index, metabolite level, and relative mRNA expression were investigated by an independent *t*-test, and the significant difference in egg production was evaluated using a one-way analysis of variance (ANOVA), followed by Duncan's multiple range test. Differences were considered statistically significant at $p < 0.05$.

3. Results and discussion

3.1. Chemical analysis

During the exposure experiment, the CBZ concentrations and other parameters, including temperature, pH, and dissolved oxygen values, in aqueous solutions, were measured. As expected, CBZ was not detected in the control groups. For the L-, M-, and H-groups, the concentrations of CBZ were comparable between day 0 and day 1 (Table S4), suggesting the stable CBZ levels in the exposure duration. The range of temperature, pH, and dissolved oxygen values were 27–28 °C, 6.5–7.5, and 5.5–7.5 mg/L, respectively (Table S5). Besides, the survival rates of zebrafish were more than 95% in all groups; this is in accordance with a previous study that CBZ was not acutely toxic because of its median lethal concentration of 8.20 mg/L towards zebrafish embryos (Richter et al., 2013). The exposure environment simulated by the present study was, therefore, suitable for zebrafish culture.

3.2. Effects on fecundity and ovarian histology

The cumulative mean egg production during both the pre-exposure (12 days) and CBZ-exposure (28 days) periods are shown in Fig. 1a. During the 12-day pre-exposure period, the egg production was consistent for all four groups, indicating a good reproductive function of zebrafish in the exposure experiment. When the zebrafish were subsequently exposed to the environmentally realistic concentration of CBZ (L-group), there was a remarkable decrease in egg production after stage 7 (12–16 days, $p < 0.05$). Exposure to higher levels of CBZ (M- and L-groups) led to an immediate reduction in egg production at stage 5 (5–8 days, $p < 0.05$). Moreover, the spawning was observed to be practically

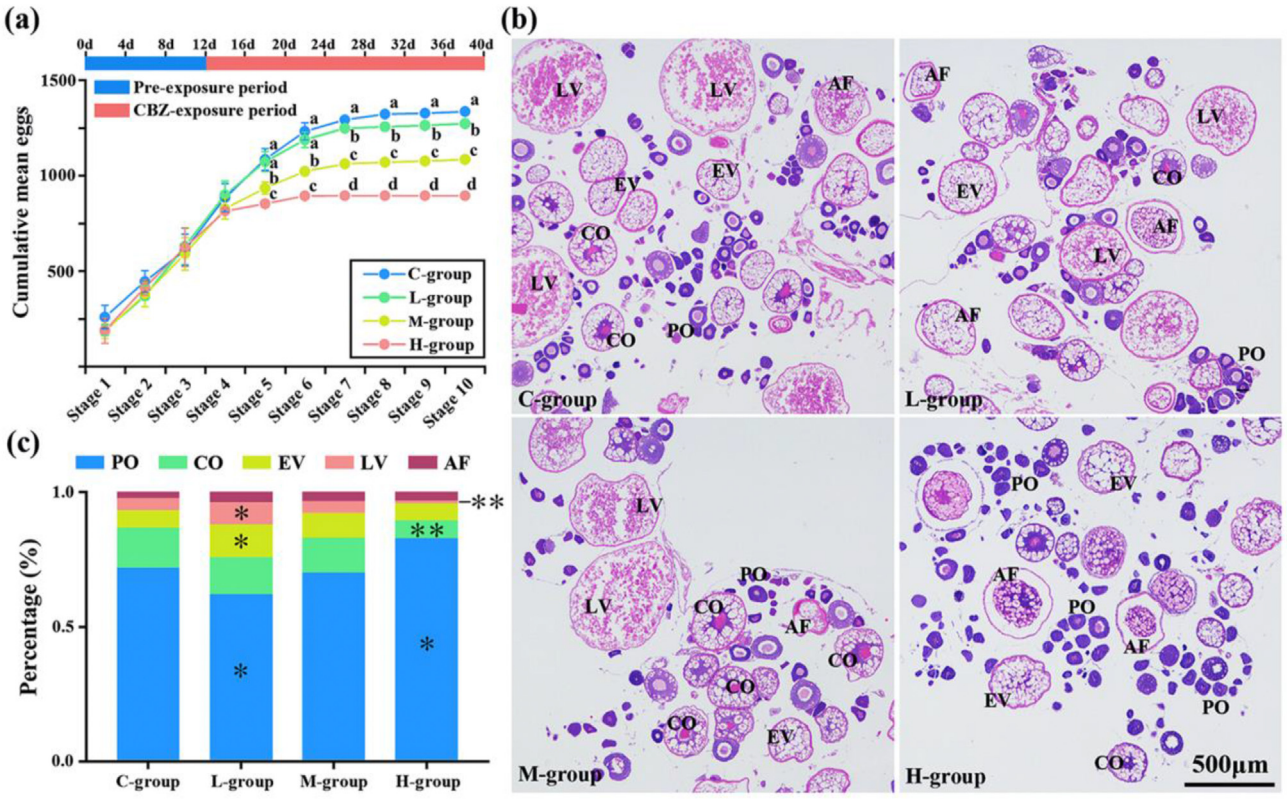

Fig. 1. Fecundity and ovarian histology of zebrafish in the C-, L-, M- and H-groups. (a) The cumulative mean number of eggs per female per 4 days in the 12-day pre-exposure period and the following 28-day exposure period. Each curve represents the mean values of four replicate tanks per 4 days per group. (b) Histological analysis of zebrafish ovaries after 28-day exposure. (c) The percentages of different developmental stages of oocytes, including perinucleolar oocytes (PO), cortical alveolar oocytes (CO), early vitellogenic oocytes (EV), late vitellogenic oocyte (LV), and atretic follicles (AF), in zebrafish ovaries after 28-day exposure. *, $p < 0.05$; **, $p < 0.01$.

stopped in the H-group. These findings reveal that increasing the exposure concentrations of CBZ will lower the egg production of zebrafish and shorten the time that occurs the significant difference of cumulative mean egg numbers between the exposure and control groups. On account of fecundity inhibition, similar results were found for fathead minnow and Japanese medaka exposed to ketoconazole and triadimenol, respectively (Ankley et al., 2007; Chu et al., 2016); however, their reported effect concentrations are much higher than the CBZ exposure concentration corresponding to its real environmental level, demonstrating that CBZ may pose high risks to fish reproduction. Accordingly, CBZ shows a concentration-dependent effect on zebrafish fecundity impairment, although it did not cause any significant changes in the body weight, ovary weight, and gonadosomatic index (Table S6).

In addition to egg production, histological alterations in ovaries were also assessed (Fig. 1b–1c). For the L-group, CBZ significantly reduced the proportion of perinucleolar oocytes but increased the percentage of early vitellogenic oocytes and late vitellogenic oocytes ($p < 0.05$), implying its promotion effect on oocyte maturation. Nevertheless, egg production was inhibited in the L-group (Fig. 1a). In the case of H-groups, a downward trend was found for the number of cortical alveolar oocytes and late vitellogenic oocytes; on the contrary, perinucleolar oocytes increased significantly. Jensen et al. noted that spawning inhibition was accompanied by a decrease in mature oocytes and an increase in atretic follicles when exposed to an antiandrogen agent (Jensen et al., 2004). In keeping with this previous study, we found that the percentage of atretic follicles in the H-group was, though not significantly, higher than that of the control group. Moreover, the decrease in cortical alveolar oocytes, early vitellogenic oocytes, and late vitellogenic oocytes and the increase in perinucleolar oocytes exhibited in a dose-dependent manner from the L-to H-groups. These findings elucidate that the reduction in fecundity posed by CBZ could be linked to retarded oocyte maturation or suppressed ovulation in zebrafish ovaries.

3.3. *Effects on ovarian metabolic profiling by untargeted metabolomics analysis*

Changes in metabolite levels are closely linked with the influence on reproductive function (Melvin et al., 2018). In order to clarify the role of key metabolites in the mechanism of CBZ-triggered toxicity, ovarian metabolome was analyzed by LC-HRMS. As shown in Fig. 2, the PLS-DA models originating from the data of positive and negative ionization modes both displayed notable separations on metabolome among the quality control (QC), solvent control (C), and all exposure (L, M, and H) groups ($R^2Y = 0.984$ and $Q^2 = 0.721$ for positive ionization mode; $R^2Y = 0.984$ and $Q^2 = 0.711$ for negative ionization mode). Combined with the volcano plots (Fig. 2), which are commonly applied for quick identification of significant up-regulation or down-regulation of endogenous metabolite levels in exposure groups versus control groups, it can be seen that CBZ could contribute conspicuous interference in ovarian metabolic profiling in a concentration-dependent manner. Next, 26 significantly changed metabolites, mainly amino acids, peptides, nucleosides, nucleotides, eicosanoids, and retinoids, between the exposure and control groups, were statistically selected and structurally identified (Table S7; Figure S1). Most biomarkers were shown to be highly associated with the disruption of retinol metabolism, glutathione

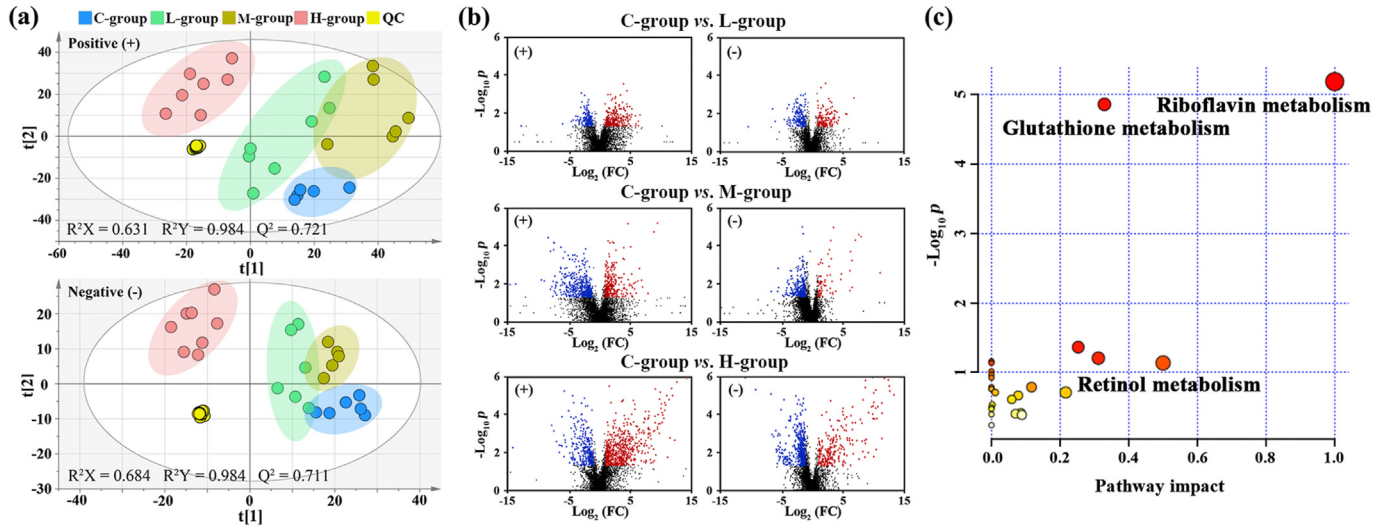

Fig. 2. Statistical analysis of metabolomics data in zebrafish ovaries. (a) PLS-DA score plots of metabolomics data in the QC-, C-, L-, M-, and H-groups in both positive and negative ionization modes. (b) Volcano plots of fold changes and significant levels of metabolites between the control and exposure groups based on both positive and negative ionization modes. Metabolites in blue circles represent FC < 0.5 and $p < 0.05$, while those in red circles denote FC > 2 and $p < 0.05$. (c) Pathway analysis of metabolomics data in the ovary of zebrafish exposed to CBZ. (For interpretation of the references to colour in this figure legend, the reader is referred to the Web version of this article.)

metabolism, and riboflavin metabolism (Fig. 2). Melvin et al. applied untargeted metabolomics to elucidate the effects on early post-hatch amphibian larvae exposed to two azole fungicides and indicated broad inhibition of endogenous metabolites, which participate in cholesterol metabolism and tricarboxylic acid cycle (Melvin et al., 2018). Although the significantly changed metabolites differ between target azoles in aquatic organisms, most previous studies found potential toxicological action sites that altered steroidogenesis and/or oxidative stress (Chu et al., 2016; Melvin et al., 2018; Zhang et al., 2019a). The details about toxicity mechanisms are discussed as follows.

3.4. Alterations in steroidogenic networks

The biosynthesis of active derivatives of retinoids (e.g., retinoic acid and retinol), involved in retinol metabolism, is crucial for physiological processes such as reproduction and vision (Clagett-Dame and DeLuca, 2002). In the gonad, retinoic acid mainly participates in premeiotic marker *Stra8* expression regulation, thereby inducing germ cells initiating meiosis (Bowles et al., 2006; Koubova et al., 2006). Most of the earlier reports indicated that interference in retinoic acid signaling could impair ovarian function, such as steroid production, follicle formation, and even ovulation, in various animal models (Alsop et al., 2008; Clagett-Dame and DeLuca, 2002; Kawai et al., 2016). Under CBZ exposure, the significant reduction of retinoic acid in zebrafish ovaries could account for a drop in egg production ($p < 0.05$; FC = 0.29–0.68; Table S8; Fig. 1).

Apart from retinoic acid, sex hormones are a class of endogenous metabolites involved in the steroidogenesis pathway, profoundly impacting on ovarian development, oocyte maturation, and reproduction in fish (Tokarz et al., 2013). Likely due to the low electrospray ionization efficiency in response to their chemical structures, sex hormones were hardly found by an untargeted mass spectrometry-based metabolomics approach. Nuclear magnetic resonance spectroscopy (NMR) did not exhibit satisfactory performance on the measurement of these endogenous steroids yet (Melvin et al., 2018). A commercially available ELISA as an alternative assay was therefore used for the detection of crucial sex hormones, including estradiol (E2), testosterone (T), and 11-ketotestosterone (11-KT). As shown in Fig. 3a, CBZ significantly reduced the 11-KT concentration in zebrafish ovaries from the L-group, while the reduction in E2 and T levels was found in all exposure groups ($p < 0.05$); this is in accordance with the findings in fathead minnow ovary explants and H295R cells exposed to most of the azole fungicides (Villeneuve et al., 2007). Moreover, we found a consistent downward trend between ovarian T or E2 levels and egg-laying capacity in female zebrafish. A similar phenomenon was observed for plasma sex hormone levels, which were reduced with the decline in egg production (Paulos et al., 2010), suggesting that CBZ causes ovarian sex hormone imbalance and, afterward, reproductive dysfunction.

As we know, the synthesis of sex hormones is primarily controlled by steroidogenic pathways; so that alternations in the transcription profiles of steroidogenesis-related genes have been

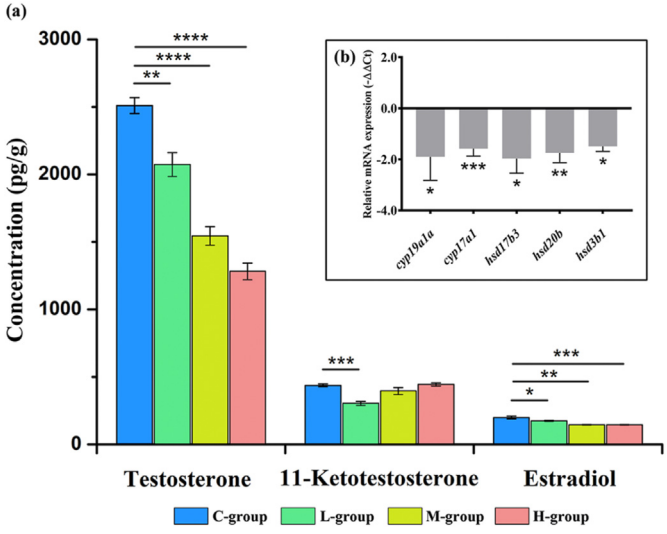

Fig. 3. (a) Concentrations of testosterone, 11-ketotestosterone and estradiol in zebrafish ovaries from different groups. (b) Relative transcription levels of steroidogenesis-related genes in zebrafish ovaries between the C- and L-groups. *, $p < 0.05$; **, $p < 0.01$; ***, $p < 0.005$; ****, $p < 0.001$.

described as the most important mechanism for endocrine disrupting chemicals (Liang et al., 2020; Shi et al., 2018). For example, the aromatase gene *cyp19a1a* involved in converting T to E2 is responsible for the prevention of oocyte apoptosis and the development of zebrafish ovaries (Uchida et al., 2002). The gene *hsd3b1* is essential for progesterone synthesis (Tokarz et al., 2013), while *hsd20b* modulates the production of 17α,20β-dihydroxy-4-pregneno-3-one (17α,20β-DHP), which is shown to be the normal inducer of fish oocyte maturation (Lessman, 2009). Brown et al. reported that exposure to an azole fungicide clotrimazole could cause male bias in inbred zebrafish, following a strong suppression of gonadal *cyp19a1a* and *hsd17b3* transcription as well as plasma 11-KT concentrations (Brown et al., 2011). In the case of CBZ, it inhibited the transcripts of *cyp19a1a* and *cyp17a1* in the early life stage of zebrafish by a large-scale screening experiment (Zhang et al., 2019a). In keeping with these earlier studies, the significant transcriptional down-regulation in female zebrafish, in response to exposure to CBZ at only real environmental concentrations (L-group), was observed for *cyp19a1a*, *cyp17a1*, as well as *hsd17b3*, *hsd20b*, and *hsd3b1* genes (Fig. 3b). This result is in accordance with the reduction in sex hormone concentrations because the essential genes *hsd17b3*, *cyp19a1a*, and *cyp17a1* modulate the production of 11-KT, E2, and androstenedione, which is the precursor of T (Tokarz et al., 2013). Given the simultaneous inhibition of RA and sex hormone concentrations and steroidogenesis-related gene transcription, we suggest that altered steroidogenesis plays a vital role in CBZ-induced reproductive toxicity (Zhang et al., 2019a), which may explain the disturbance in oogenesis in zebrafish ovaries.

3.5. Induction of apoptosis

Apart from retinol metabolism, metabolomics analysis indicated that CBZ had remarkable effects on glutathione metabolism and riboflavin metabolism (Fig. 2), presumably leading to oxidative stress and even apoptosis. A brief glutathione biosynthetic pathway is shown in Fig. 4a. Glutamate and the dipeptide gamma-glutamylcysteine (γGluCys) were observed to decrease in the exposure group (Fig. 4a), suggesting the disturbance in glutathione biosynthesis, in which they are used as precursors (Lu, 2013). It is well known that the glutathione, existing in reduced (GSH) and oxidized (GSSG) states, is an antioxidant for cellular defense against reactive oxygen species (Wu et al., 2004). When oxidative stress occurs, the conversion of GSH to GSSG starts to prevent damages; so that the ratio of GSSG to GSH is an important indicator of cellular oxidative stress (Lu, 2013). Because of a significant increase in GSSG ($p < 0.05$; FC = 3.92 and 1.77), CBZ showed a slight induction of oxidative stress in zebrafish ovaries from the L- and M-groups, whereas GSH remained unchanged (Fig. 4a). It can be explained by the immediate replenishment of GSH from the upstream metabolites, resulting in the consumption of glutamate or γGluCys. For the H-group, the GSSG/GSH increased the most and thereby showed a concentration-dependent effect. These results provide evidence of the occurrence of ovarian oxidative stress in zebrafish exposed to CBZ. Most importantly, GSH was observed to be basically depleted ($p < 0.01$, FC = 0.33) for the following reasons. On the one hand, its downstream metabolite GSSG seemed to increase, though not significantly ($p > 0.05$), while the levels were lower in the H-group than the L-group. On the other hand, we found that cysteine-glutathione disulfide (CYSSG) produced endogenously via a thiol-disulfide exchange reaction from GSH (Eriksson and Eriksson, 1967) increased with the increasing CBZ exposure concentration.

Besides, the abnormality in riboflavin metabolism was induced by CBZ exposure (Fig. 2). Based on the KEGG pathway database, the metabolic pathway involves converting riboflavin to flavin adenine dinucleotide (FAD) via an intermediate product flavin mononucleotide (FMN). It was reported that riboflavin plays a key role in GSH regeneration because glutathione reductase (GR) needs to combine with the redox-active coenzyme FAD to exert its physiological function (Beutler, 1969). The reduction in riboflavin and FMN led to the gradually increasing FAD after exposure to CBZ (Fig. 4a). Combined with the increasing $NADP^+$, these findings reveal that stimulating the GR activity and promoting GSH regeneration were the negative feedback regulation to resist oxidative damages (Beutler, 1969). However, triggering GSH regeneration could not maintain GSH homeostasis for the H-group, probably due to the greater oxidative damage (Lu, 2013). Melvin et al. demonstrated oxidative stress by azole fungicides based on the broad down-regulation of the tricarboxylic acid cycle (Melvin et al., 2018). Although the differences in signaling pathways, oxidative stress was found to be induced by CBZ (Zhang et al., 2019a).

Moreover, GSH deficiency will enhance cellular reactive oxygen species (ROS) and induce the DNA strand breaks (Esteve et al., 1999; Morel and Barouki, 1999). There is growing evidence for the close correlation between oxidative stress and cell apoptosis (Kannan and Jain, 2000). In the present study, a TUNEL assay was used to identify apoptotic cells (Magnuson et al., 2020). As shown in Fig. 4b, apoptotic cells were found in the zebrafish ovarian tissue sections from the L-, M-, and H-groups but not in the control group. Our findings are consistent with the previous studies for an aromatase inhibitor fadrozole (Luzio et al., 2016; Uchida et al., 2004). For the L-group, slight oocyte apoptosis reveals that CBZ has apoptosis-induced capacity even at real environmental concentrations. The most interesting finding was that oocyte apoptosis in the H-group was not as severe as that in the M-group, which may be attributed to cell necrosis in the H-group. Higuchi indicated that the change from apoptosis to necrosis might depend on the intensity of oxidative stress (Higuchi, 2004). Slight or moderate oxidation can initiate apoptosis, while more intense stress may lead to necrosis (Lennon et al., 1991). In the case of GSH depletion, the release of arachidonic acid (AA) will be enhanced (Samanta et al., 1998), and high concentrations of AA turn apoptosis into necrosis (Higuchi and Yoshimoto, 2004). In keeping with these previous reports, we found AA enhancement and GSH depletion in the H-group (Table S8) to support the idea that cell necrosis partly instead of cell apoptosis occurred and was thought to be detrimental to the zebrafish ovary, such as the delay in ovarian development and the impairment of reproduction (Luzio et al., 2016).

In addition to AA enhancement, other differential metabolites, including eicosapentaenoic acid (EPA), 5-hydroxyeicosapentaenoic acid (5-HEPE), and lipoxin A_4 (LXA_4), involved in the anti-inflammatory response (Lee et al., 1985; Lv et al., 2013), were found to decrease significantly ($p < 0.05$, FC = 0.21–0.55) in the exposure groups (Table S8; Figure S2), suggesting that exposure to CBZ could induce inflammatory response; this is consistent with the findings of our earlier study for zebrafish eleutheroembryos (Zhang et al., 2019a). Interestingly, LXA_4 not only acts to resolve inflammatory responses but also has the ability to promote GSH release and reduce oxidative stress (Wu et al., 2015). Forrester et al. summarized sufficient evidence pointing to a role for ROS in the regulation of inflammatory signaling (Forrester et al., 2018). It seems reasonable to suppose that inflammation and oxidative stress are interconnected contribution to the reproductive dysfunction induced by CBZ, yet the mechanism remains somewhat elusive.

In order to confirm the variation of vital differential metabolites induced by CBZ, the ovarian tissues in whole zebrafish sections from the control and exposure groups were analyzed by an emerging technique MALDI-MSI (Zhao et al., 2018; 2020a). In the present study, the use of the whole zebrafish sagittal tissue section, including ovaries, rather than isolation of ovarian follicles, gains an

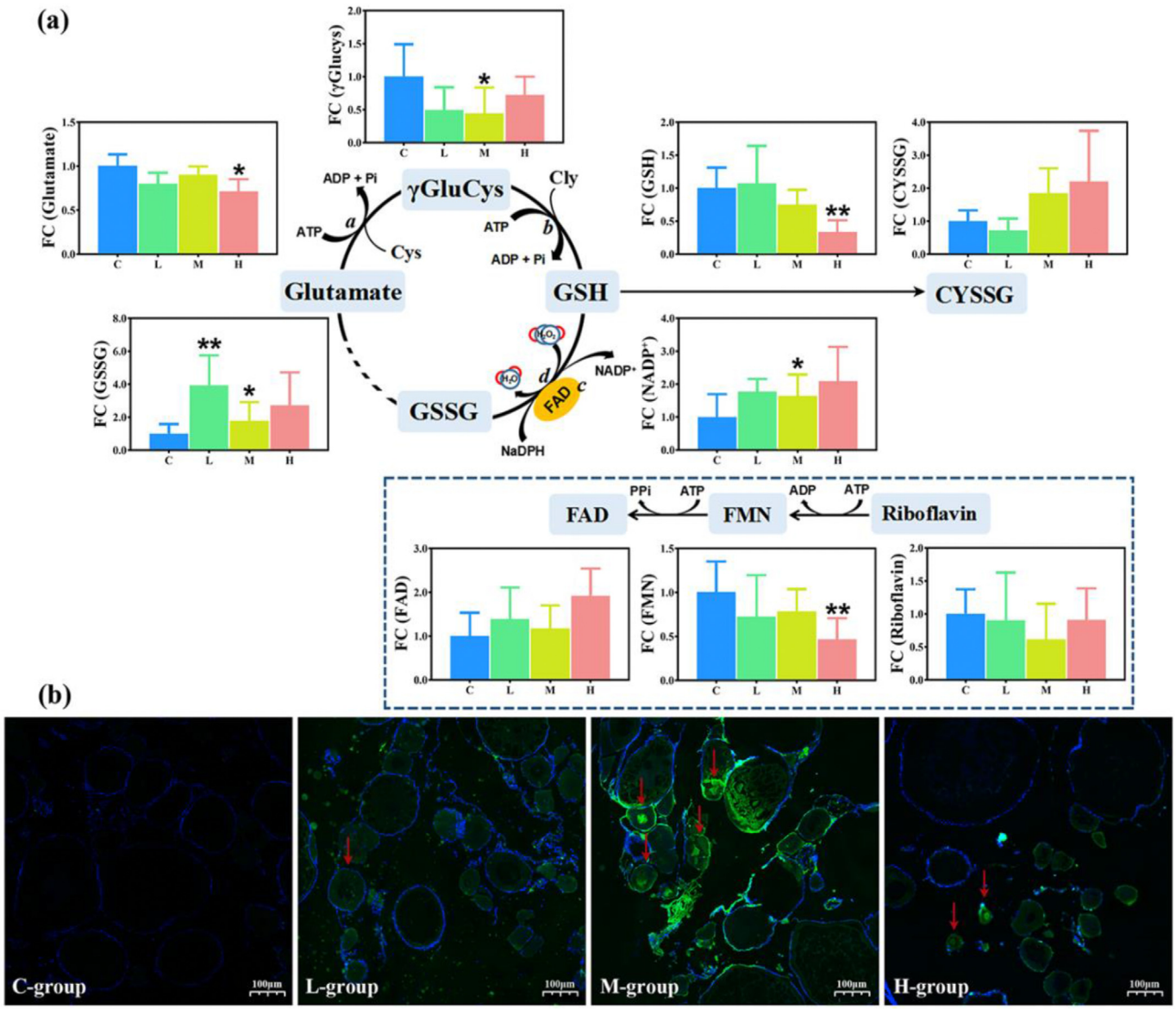

Fig. 4. (a) Changes of identified metabolites involved in glutathione metabolism and riboflavin metabolism in zebrafish ovaries between the control and exposure groups. a, γ-GluCys synthetase; b, glutathione synthetase; c, GR, glutathione reductase; d, GSH-Px, glutathione peroxidase. *, $p < 0.05$; **, $p < 0.01$. (b) TUNEL labeling (green) in zebrafish ovaries from different groups (scale bar 100 μm). (For interpretation of the references to colour in this figure legend, the reader is referred to the Web version of this article.)

advantage of the visual judgment of metabolite variation but leads to difficulty in observing spatial distribution of metabolites in the ovary. Additionally, box plots displaying the normalized intensity of each metabolite from overall spectra were applied to distinguish digitally. The characteristic peaks at m/z 330.074 ± 0.112, 635.142 ± 0.112, and 465.052 ± 0.112 were assigned to GSH, GSSG, and CYSSG, respectively. Similar to the findings from metabolomics analysis, down-regulated GSH was shown in the H-group, while GSSG and CYSSG gradually increased from the C-, L-, M- to H-groups (Fig. 5). The identified glutathione-related metabolites could serve as imaging markers for the implication of oxidative stress (Eriksson and Eriksson, 1967; Lu, 2013). Images from AA (m/z 305.248 ± 0.112), EPA (m/z 341.188 ± 0.112), and LXA_4 (m/z 353.233 ± 0.112) show different abundance in the exposure group compared to the control group (Figure S3). Up-regulated AA and down-regulated EPA and LXA_4 are suggestive of pro-inflammatory response (Lee et al., 1985; Lv et al., 2013), which is consistent with the results of metabolomics analysis. Therefore, MALDI-MSI could be a promising tool for the validation of metabolomics results.

4. Conclusions and environmental implications

Based on the obtained results, two possible mechanisms of CBZ-induced reproductive toxicity are proposed as follows. On the one hand, CBZ down-regulates the transcriptional expression of steroidogenic cytochrome P450 genes and the endogenous level of sex hormones as well as RA. On the other hand, CBZ acting as a xenobiotic is thought to be metabolized with the involvement of GSH and thus triggers the oxidative stress and inflammatory response. The disturbance in glutathione metabolism and riboflavin metabolism exacerbates oxidative damage and further induces apoptosis and even necrosis. As a result, the reduction in egg production was observed. Our findings provide direct evidence of reproductive dysfunction in female zebrafish after chronic

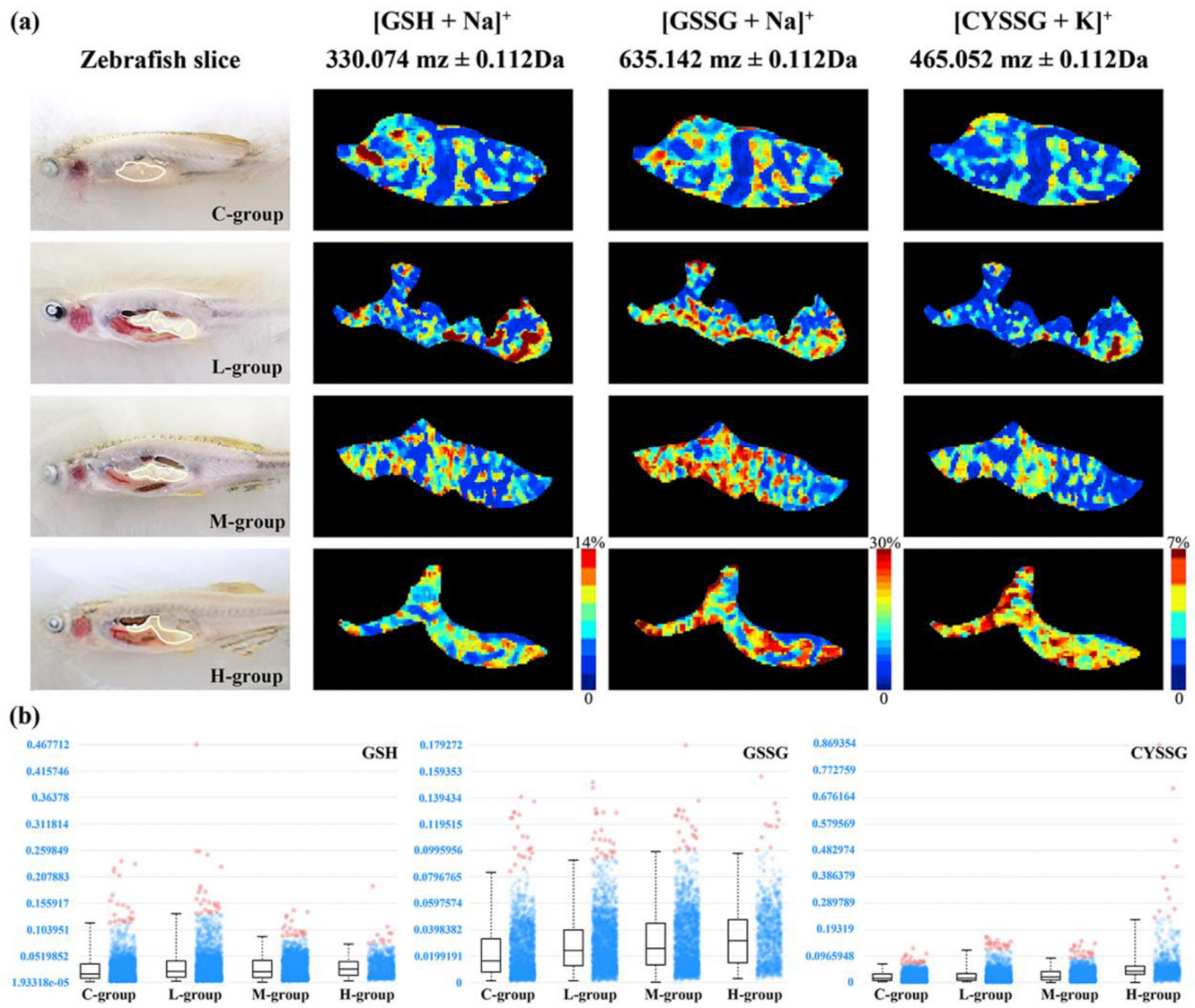

Fig. 5. MALDI-MSI analysis of differential metabolites involved in glutathione metabolism in zebrafish ovary tissue sections. (a) Optical image of the whole zebrafish sagittal slice and imaging of metabolites in zebrafish ovary tissue sections. The intensity scale is an arbitrary relative scale ranging from blue (lowest) to red (highest); (b) Box plots of metabolite intensities in the control and exposure groups. (For interpretation of the references to colour in this figure legend, the reader is referred to the Web version of this article.)

exposure to environmentally realistic concentrations of CBZ, corroborating that CBZ is an endocrine disruptor and has an ecological impact on fish reproduction to a certain extent. The pervasiveness of CBZ in the aquatic environment should (Chen and Ying, 2015), therefore, raise increasing concerns. Moreover, MALDI-MSI was used to confirm the results of metabolomics analysis, indicating that the comprehensive methodology combined metabolome study and imaging analysis is beneficial for exploring the in-depth mechanisms of metabolic disorders induced by environmental pollutants.

Contributors

Ting Zou, designed the experiments, conducted the fish exposure experiment, performed the metabolomics analysis, performed the histological examination, conducted sex hormone measurement, conducted the TNUEL assay, conducted the MALDI-MSI analysis, wrote the paper. Yan-Qiu Liang, designed the experiments, performed the histological examination, performed the RT-qPCR analysis, wrote the paper. Xiaoliang Liao, performed the metabolomics analysis. Xiao-Fan Chen, conducted the fish exposure experiment, performed the RT-qPCR analysis. Tao Wang, conducted the MALDI-MSI analysis. Yuanyuan Song, performed the metabolomics analysis. Zhi-Cheng Lin, conducted the fish exposure experiment, conducted sex hormone measurement. Zenghua Qi, performed the RT-qPCR analysis. Zhi-Feng Chen, designed the experiments, performed the metabolomics analysis, conducted the MALDI-MSI analysis, wrote the paper. Zongwei Cai, designed the experiments, wrote the paper, All authors discussed and commented on the manuscript and approved the manuscript to be submitted.

Declaration of competing interest

The authors declare no competing financial interest.

Acknowledgments

We would be grateful for the financial support from the National Natural Science Foundation of China (21507163 and 41907346), Guangdong Provincial Key Laboratory of Chemical Pollution and Environmental Safety (2019B030301008), and National Key Research and Development Project (2019YFC1804604).

Appendix A. Supplementary data

Supplementary data to this article can be found online at https://doi.org/10.1016/j.envpol.2021.116665.

References

Alsop, D., Matsumoto, J., Brown, S., Kraak, G.V.D., 2008. Retinoid requirements in the reproduction of zebrafish. Gen. Comp. Endocrinol. 156, 51–62.
Ankley, G.T., Jensen, K.M., Kahl, M.D., Makynen, E.A., Blake, L.S., Greene, K.J., Johnson, R.D., Villeneuve, D.L., 2007. Ketoconazole in the fathead minnow (*Pimephales promelas*): reproductive toxicity and biological compensation. Environ. Toxicol. Chem. 26, 1214–1223.
Beutler, E., 1969. Effect of flavin compounds on glutathione reductase activity: *In vivo* and *in vitro* studies. J. Clin. Invest. 48, 1957–1966.
Bowles, J., Knight, D., Smith, C., Wilhelm, D., Richman, J., Mamiya, S., Yashiro, K., Chawengsaksophak, K., Wilson, M.J., Rossant, J., Hamada, H., Koopman, P., 2006. Retinoid signaling determines germ cell fate in mice. Science 312.
Brown, A.R., Bickley, L.K., Le Page, G., Hosken, D.J., Paull, G.C., Hamilton, P.B., Owen, S.F., Robinson, J., Sharpe, A.D., Tyler, C.R., 2011. Are toxicological responses in laboratory (Inbred) zebrafish representative of those in outbred (Wild) populations? - a case study with an endocrine disrupting chemical. Environ. Sci. Technol. 45, 4166–4172.
Chen, Z.F., Ying, G.G., 2015. Occurrence, fate and ecological risk of five typical azole fungicides as therapeutic and personal care products in the environment: a review. Environ. Int. 84, 142–153.
Chen, Z.F., Ying, G.G., Lai, H.J., Chen, F., Su, H.C., Liu, Y.S., Peng, F.Q., Zhao, J.L., 2012. Determination of biocides in different environmental matrices by use of ultra-high-performance liquid chromatography-tandem mass spectrometry. Anal. Bioanal. Chem. 404, 3175–3188.
Chen, Z.F., Ying, G.G., Liu, Y.S., Zhang, Q.Q., Zhao, J.L., Liu, S.S., Chen, J., Peng, F.J., Lai, H.J., Pan, C.G., 2014. Triclosan as a surrogate for household biocides: an investigation into biocides in aquatic environments of a highly urbanized region. Water Res. 58, 269–279.
Chu, S.H., Liao, P.H., Chen, P.J., 2016. Developmental exposures to an azole fungicide triadimenol at environmentally relevant concentrations cause reproductive dysfunction in females of medaka fish. Chemosphere 152, 181–189.
Clagett-Dame, M., DeLuca, H.F., 2002. The role of vitamin A in mammalian reproduction and embryonic development. Annu. Rev. Nutr. 22, 347–381.
ECHA, 2013. Justification for the selection of a candidate CoRAP substance (climbazole). Available from: https://echa.europa.eu/documents/10162/10104ac10108fa-10137d10166-10165ffd-10109a-f10112c14785e10111e.
Eriksson, B., Eriksson, S.A., 1967. Synthesis and characterization of the L-cysteine-glutathione mixed disulfide. Acta Chem. Scand. 21, 1304–1312.
Esteve, J.M., Mompo, J., Garcia de la Asuncion, J., Sastre, J., Asensi, M., Boix, J., Vina, J.R., Vina, J., Pallardó, F.V., 1999. Oxidative damage to mitochondrial DNA and glutathione oxidation in apoptosis: studies *in vivo* and *in vitro*. Faseb. J. 13, 1055–1064.
Fiehn, O., 2002. Metabolomics – the link between genotypes and phenotypes. Plant Mol. Biol. 48, 155–171.
Forrester, S.J., Kikuchi, D.S., Hernandes, M.S., Xu, Q., Griendling, K.K., 2018. Reactive oxygen species in metabolic and inflammatory signaling. Circ. Res. 122, 877–902.
Higuchi, Y., 2004. Glutathione depletion-induced chromosomal DNA fragmentation associated with apoptosis and necrosis. J. Cell Mol. Med. 8, 455–464.
Higuchi, Y., Yoshimoto, T., 2004. Promoting effects of polyunsaturated fatty acids on chromosomal giant DNA fragmentation associated with cell death induced by glutathione depletion. Free Radic. Res. 38, 649–658.
Jensen, K.M., Kahl, M.D., Makynen, E.A., Korte, J.J., Leino, R.L., Butterworth, B.C., Ankley, G.T., 2004. Characterization of responses to the antiandrogen flutamide in a short-term reproduction assay with the fathead minnow. Aquat. Toxicol. 70, 99–110.
Jiang, Y.X., Shi, W.J., Ma, D.D., Zhang, J.N., Ying, G.G., Zhang, H., Ong, C.N., 2019. Dydrogesterone exposure induces zebrafish ovulation but leads to oocytes over-ripening: an integrated histological and metabolomics study. Environ. Int. 128, 390–398.
Kannan, K., Jain, S.K., 2000. Oxidative stress and apoptosis. Pathophysiology 7, 153–163.
Kawai, T., Yanaka, N., Richards, J.S., Shimada, M., 2016. De novo-synthesized retinoic acid in ovarian antral follicles enhances FSH-mediated ovarian follicular cell differentiation and female fertility. Endocrinology 157, 2160–2172.
Koubova, J., Menke, D.B., Zhou, Q., Capel, B., Griswold, M.D., Page, D.C., 2006. Retinoic acid regulates sex-specific timing of meiotic initiation in mice. P. Natl. Acad. Sci. USA 103, 2474–2479.
Lee, T.H., Hoover, R.L., Williams, J.D., Sperling, R.I., Austen, K.F., 1985. Effect of dietary enrichment with eicosapentaenoic and docosahexaenoic acids on *in vitro* neutrophil and monocyte leukotriene generation and neutrophil function. N. Engl. J. Med. 312, 1217–1224.
Lennon, S.V., Martin, S.J., Cotter, T.G., 1991. Dose-dependent induction of apoptosis in human tumour cell lines by widely diverging stimuli. Cell Prolif 24, 203–214.
Lessman, C.A., 2009. Oocyte maturation: converting the zebrafish oocyte to the fertilizable egg. Gen. Comp. Endocrinol. 161, 53–57.
Liang, Y.Q., Jing, Z., Pan, C.G., Lin, Z., Zhen, Z., Hou, L., Dong, Z., 2020. The progestin norethindrone alters growth, reproductive histology and gene expression in zebrafish (*Danio rerio*). Chemosphere 242, 125285.
Liao, P.H., Chu, S.H., Tu, T.Y., Wang, X.H., Lin, A.Y., Chen, P.J., 2014. Persistent endocrine disruption effects in medaka fish with early life-stage exposure to a triazole-containing aromatase inhibitor (letrozole). J. Hazard Mater. 277, 141–149.
Liu, W.R., Yang, Y.Y., Liu, Y.S., Zhang, L.J., Zhao, J.L., Zhang, Q.Q., Zhang, M., Zhang, J.N., Jiang, Y.X., Ying, G.G., 2017. Biocides in wastewater treatment plants: mass balance analysis and pollution load estimation. J. Hazard Mater. 329, 310–320.
Livak, K.J., Schmittgen, T.D., 2001. Analysis of relative gene expression data using real-time quantitative PCR and the $2^{-\Delta\Delta CT}$ method. Methods 25, 402–408.
Lu, S.C., 2013. Glutathione synthesis. Biochim. Biophys. Acta 1830, 3143–3153.
Luzio, A., Matos, M., Santos, D., Fontainhas-Fernandes, A.A., Monteiro, S.M., Coimbra, A.M., 2016. Disruption of apoptosis pathways involved in zebrafish gonad differentiation by 17α-ethinylestradiol and fadrozole exposures. Aquat. Toxicol. 177, 269–284.
Lv, W., Lv, C., Yu, S., Yang, Y., Kong, H., Xie, J., Sun, H., Andersson, R., Xu, D., Chen, B., Zhou, M., 2013. Lipoxin A4 attenuation of endothelial inflammation response mimicking pancreatitis-induced lung injury. Exp. Biol. Med. 238, 1388–1395.
Magnuson, J.T., Bautista, N.M., Lucero, J., Lund, A.K., Xu, E.G., Schlenk, D., Burggren, W.W., Roberts, A.P., 2020. Exposure to crude oil induces retinal apoptosis and impairs visual function in fish. Environ. Sci. Technol. 54, 2843–2850.
Melvin, S.D., Leusch, F.D.L., Carroll, A.R., 2018. Metabolite profiles of striped marsh frog (*Limnodynastes peronii*) larvae exposed to the anti-androgenic fungicides vinclozolin and propiconazole are consistent with altered steroidogenesis and oxidative stress. Aquat. Toxicol. 199, 232–239.
Morel, Y., Barouki, R., 1999. Repression of gene expression by oxidative stress. Biochem. J. 342, 481–496.
Paulos, P., Runnalls, T.J., Nallani, G., Point, T.L., Scott, A.P., Sumpter, J.P., Huggett, D.B., 2010. Reproductive responses in fathead minnow and Japanese medaka following exposure to a synthetic progestin. Norethindrone. Aquat. Toxicol. 99, 256–262.
Richter, E., Wick, A., Ternes, T.A., Coors, A., 2013. Ecotoxicity of climbazole, a fungicide contained in antidandruff shampoo. Environ. Toxicol. Chem. 32, 2816–2825.
Samanta, S., Perkinton, M.S., Morgan, M., Williams, R.J., 1998. Hydrogen peroxide enhances signal-responsive arachidonic acid release from neurons: role of mitogen-activated protein kinase. J. Neurochem. 70, 2082–2090.
SCCS, 2017. Addendum to the Opinion on Climbazole (P64) Ref. SCCS/1506/13, pp. 24–25. SCCS/1590/17. Available from: https://hal.archives-ouvertes.fr/hal-01650396/document.
Shi, W.J., Jiang, Y.X., Huang, G.Y., Zhao, J.L., Zhang, J.N., Liu, Y.S., Xie, L., Ying, G.G., 2018. Dydrogesterone causes male bias and accelerates sperm maturation in zebrafish (*Danio rerio*). Environ. Sci. Technol. 52, 8903–8911.
Teng, M., Zhu, W., Wang, D., Qi, S., Wang, Y., Yan, J., Dong, K., Zheng, M., Wang, C., 2018. Metabolomics and transcriptomics reveal the toxicity of difenoconazole to the early life stages of zebrafish (*Danio rerio*). Aquat. Toxicol. 194, 112–120.
Tokarz, J., Moller, G., Angelis, M.H., Adamski, J., 2013. Zebrafish and steroids: what do we know and what do we need to know? J. Steroid Biochem. 137, 165–173.
Uchida, D., Yamashita, M., Kitano, T., Iguchi, T., 2002. Oocyte apoptosis during the transition from ovary-like tissue to testes during sex differentiation of juvenile zebrafish. J. Exp. Biol. 205, 711–718.
Uchida, D., Yamashita, M., Kitano, T., Iguchi, T., 2004. An aromatase inhibitor or high water temperature induce oocyte apoptosis and depletion of P450 aromatase activity in the gonads of genetic female zebrafish during sex-reversal. Comp. Biochem. Physiol. A 137, 11–20.
Villeneuve, D.L., Ankley, G.T., Makynen, E.A., Blake, L.S., Greene, K.J., Higley, E.B., Newsted, J.L., Giesy, J.P., Hecker, M., 2007. Comparison of fathead minnow ovary explant and H295R cell-based steroidogenesis assays for identifying endocrine-active chemicals. Ecotoxicol. Environ. Saf. 68, 20–32.
Wei, W.W., Zhong, Y., Zou, T., Chen, X.F., Ren, L., Qi, Z., Liu, G., Chen, Z.F., Cai, Z., 2020. Fe_3O_4-assisted laser desorption ionization mass spectrometry for typical metabolite analysis and localization: influencing factors, mechanisms, and environmental applications. J. Hazard Mater. 388, 121817.
Wu, G., Fang, Y.Z., Yang, S., Lupton, J.R., Turner, N.D., 2004. Glutathione metabolism and its implications for health. J. Nutr. 134, 489–492.
Wu, L., Li, H.H., Wu, Q., Miao, S., Liu, Z.J., Wu, P., Ye, D.Y., 2015. Lipoxin A_4 activates Nrf2 pathway and ameliorates cell damage in cultured cortical astrocytes exposed to oxygen-glucose deprivation/reperfusion insults. J. Mol. Neurosci. 56, 848–857.
Yan, S.C., Chen, Z.F., Zhang, H., Chen, Y., Qi, Z., Liu, G., Cai, Z., 2020. Evaluation and optimization of sample pretreatment for GC/MS-based metabolomics in embryonic zebrafish. Talanta 207, 120260.

Zhang, H., Chen, Z.F., Qi, Z., Yan, S.C., Wei, W.W., Liu, G., Cai, Z., 2019a. Analysis of transcriptional response in zebrafish eeutheroembryos exposed to climbazole: signaling pathways and potential biomarkers. Environ. Toxicol. Chem. 38, 794–805.
Zhang, H., Shao, X., Zhao, H., Li, X., Wei, J., Yang, C., Cai, Z., 2019b. Integration of metabolomics and lipidomics reveals metabolic mechanisms of triclosan-induced toxicity in human hepatocytes. Environ. Sci. Technol. 53, 5406–5415.
Zhang, Q.Q., Ying, G.G., Chen, Z.F., Liu, Y.S., Liu, W.R., Zhao, J.L., 2015. Multimedia fate modeling and risk assessment of a commonly used azole fungicide climbazole at the river basin scale in China. Sci. Total Environ. 520, 39–48.
Zhao, C., Xie, P., Yong, T., Huang, W., Liu, J., Wu, D., Ji, F., Li, M., Zhang, D., Li, R., Dong, C., Ma, J., Dong, Z., Liu, S., Cai, Z., 2020a. Airborne fine particulate matter induces cognitive and emotional disorders in offspring mice exposed during pregnancy. Sci. Bull. doi.org/10.1016/j.scib.2020.08.036.
Zhao, C., Xie, P., Yong, T., Wang, H., Chung, A.C.K., Cai, Z., 2018. MALDI-MS imaging reveals asymmetric spatial distribution of lipid metabolites from bisphenol S-induced nephrotoxicity. Anal. Chem. 90, 3196–3204.
Zhao, C., Yong, T., Zhang, Y., Jin, Y., Xiao, Y., Wang, H., Zhao, B., Cai, Z., 2020b. Evaluation of the splenic injury following exposure of mice to bisphenol S: a mass spectrometry-based lipidomics and imaging analysis. Environ. Int. 135, 105378.